Regulation of Turbulent Transport in Neoclassically Optimized Helical Configurations with Radial Electric Fields

T.-H.Watanabe[1,2], H.Sugama[1,2], and S. Ferrando-Margalet[1]

[1]National Institute for Fusion Science / [2]The Graduate University for Advanced Studies, Toki, Gifu, 509-5929, Japan

e-mail contact of main author: watanabe.tomohiko@nifs.ac.jp

Abstract. Gyrokinetic Vlasov simulations of the ion temperature gradient turbulence demonstrate reduction of the turbulent transport with enhanced zonal-flow generation in the neoclassically optimized helical configuration as predicted by the theoretical analysis of the zonal-flow response. The inward-shifted plasma of the Large Helical Device, thus, has better confinement than that with the standard magnetic axis position, which is consistent with the experimental results. The zonal-flow response is also investigated for case with the equilibrium radial electric field that can be generated by the ambipolar neoclassical particle transport in helical systems. The gyrokinetic theory and simulation clarify that the poloidal $\boldsymbol{E} \times \boldsymbol{B}$ rotation of the helically trapped particles enhances the zonal flow response which can lead to further reduction of the turbulent transport.

1. Introduction

The ion temperature gradient (ITG) turbulence [1] and the zonal flows [2] are important ingredients for considering the anomalous ion heat transport in magnetically confined fusion plasmas. Gyrokinetic theories and simulations [3] on the zonal flows and the ITG turbulence deepen comprehension of the anomalous transport mechanism. Among them, the theory of zonal flows developed by Rosenbluth and Hinton [4] has provided us a quantitative evaluation of the response function to a given turbulent source. It is demonstrated by the gyrokinetic Vlasov (GKV) simulation [5] that the Landau damping process of the zonal flow and the geodesic acoustic mode (GAM) oscillations [6] are closely related to fine oscillatory velocity-space structures of the perturbed ion gyrocenter distribution function, δf. Also, a coherent structure of δf associated with the residual zonal flow [4] is clearly identified in the GKV simulation.

The gyrokinetic theory on the zonal flow and GAM driven by the ITG turbulence has been extended to helical systems [7–9] as a generalization of the work in Ref. [4] for tokamaks. The theoretical and computational analyses show that a high-level zonal flow can be maintained for a longer time by reducing bounce-averaged radial drift velocity of helical-ripple-trapped particles. This means that optimization of the three-dimensional magnetic configuration for reducing the neoclassical ripple transport can simultaneously increase the residual zonal flows which are expected to lower the anomalous transport. [7–10]. It is actually observed in the Large Helical Device (LHD) [11] experiments that the anomalous transport decreases in the inward-shifted plasma configuration optimized for reducing the neoclassical transport [12].

This paper is organized as follows. The gyrokinetic simulations of ITG turbulence relevant to the LHD experimental conditions are described in the next section, where the ion heat transport reduction by the zonal-flow enhancement is presented. Recent extensions of theory and simulation of the zonal-flow response to the case with the equilibrium radial electric field are summarized in sections 3.1 and 3.2. The new GKV simulation results are shown in section 3.3. A summary is given in the last section.

2. Gyrokinetic Simulation of ITG Turbulence in LHD Configurations

Our previous simulations of the ITG turbulence and the zonal flows in helical systems [13] demonstrated stronger generation of zonal flows in a model configuration for the inward-shifted

LHD plasma, while the obtained ion heat transport in the inward-shifted case was higher than that in the standard one in contrast to the LHD experimental results. This is attributed to remarkably larger growth rates of the ITG mode in the inward-shifted case. Also, the stationary zonal-flow structure effectively regulating the turbulent transport was not clearly observed in the simulations. In our recent study [9] on the linear ITG stability and the zonal-flow response for the inward-shifted and standard configurations relevant to the LHD experiments, it is found that stabilizing effects of the smaller safety factor and the stronger magnetic shear associated with the inward plasma shift decrease the difference of the ITG mode growth rates between the two cases. Also, specified changes in the helical field components, the safety factor, and the aspect ratio show that an initially given zonal flow keeps a higher level for a longer time in the inward-shifted configuration than that in the standard one. In this section, we describe results of our recent nonlinear GKV simulation implemented with the relevant magnetic field parameters where we could confirm generation of large zonal flows enough to reduce the ion heat transport in the inward-shifted plasma [14].

2.1. Simulation Model

By using the GKV code [5, 13], we numerically solve the nonlinear gyrokinetic equation [15] for the perturbed ion distribution function, δf, in the low-β electrostatic limit with the assumption of a large-aspect-ratio torus. The equilibrium background component of ions are assumed to be Maxwellian F_M. We employed the Lenard-Bernstein collision term, $C(\delta f)$. The toroidal flux tube model [16] with the field-aligned coordinates of $x = r - r_0$, $y = \frac{r_0}{q_0}[q(r)\theta - \zeta]$, and $z = \theta$ is applied in the GKV code for the ITG turbulence simulation, where $q(r)$ stands for the safety factor, and $q_0 = q(r_0)$.

In application of the GKV code to the helical system, we have introduced the equilibrium model for the LHD plasmas as given below. The averaged minor radius, r_0, is defined by $\Psi_t = \pi B_0 r_0^2$ where Ψ_t means the toroidal flux. The toroidal and helical effects of the confinement field are introduced by the change of magnetic field strength,

$$B = B_0 \left\{ 1 - \varepsilon_{00}(r) - \varepsilon_t(r)\cos z - \sum_{l=L-1}^{l=L+1} \varepsilon_l(r)\cos[(l - Mq_0)z - M\alpha] \right\}, \qquad (1)$$

where the parameters representing the toroidicity and helicity are assumed to be small, such that $\varepsilon_t = r_0/R_0 \ll 1$ and $|\varepsilon_l| \ll 1$, respectively. The major radius is denoted by R_0. The poloidal and toroidal periodicities of the helical field are represented by L and M. For LHD, $L = 2$ and $M = 10$. The averaged normal curvature is also taken into account such that $\varepsilon'_{00} = d\varepsilon_{00}/dr$ [17]. We consider major side band helical components of ε_{L-1} and ε_{L+1}. The detailed parameters of ε_{00}, ε_t, ε_l and their radial derivatives relevant to the LHD experiments are introduced in Ref. [9] for the inward-shifted and standard configurations. We also set the field-line label α to be constant ($\alpha = 0$) because the local analysis of the linear ITG instability in helical systems shows the weak dependence on α [18]. See Ref. [5, 9, 13] for more details of the GKV code and its application to the helical configurations.

2.2 Simulation Results

As shown in the previous subsection, magnetic configuration models relevant to the LHD experiments with the inward-shifted and standard plasma positions [9] are employed in the GKV code for simulating the ITG turbulent transport and zonal-flow generation. We carried out the ITG turbulence simulations for the two model configurations [14]. Color contours of the

electrostatic potential ϕ in the steady ITG turbulence are plotted in Fig. 1, where the collision frequency is negligibly smaller than the linear ITG mode growth rates. The ballooning-type mode structure of the ITG instability observed in the linear growth phase is destroyed in the latter turbulent state by the self-generated zonal flows. For the inward-shifted configuration shown in Fig. 1 (left), we see clear structures of poloidal $\boldsymbol{E} \times \boldsymbol{B}$ zonal flows in the potential profile mapped on the poloidal cross section, while more isotropic $\boldsymbol{E} \times \boldsymbol{B}$ vortices are observed in the standard case [see Fig. 1 (right)].

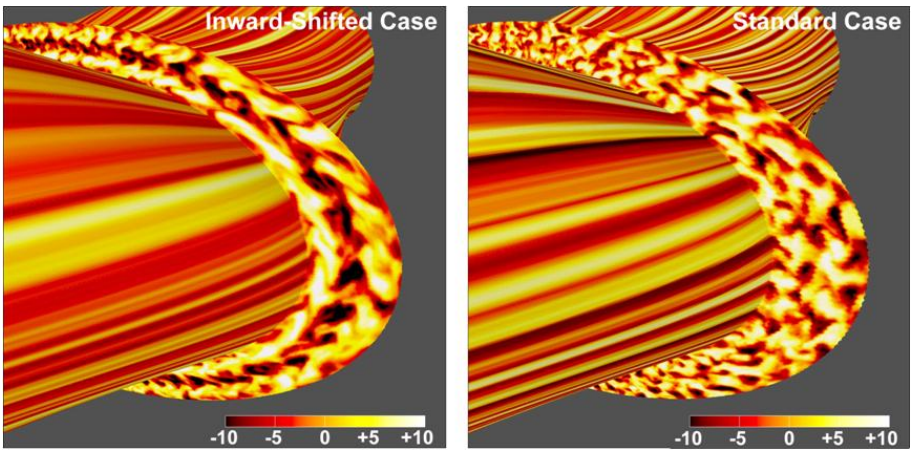

FIG. 1: Color Contours of the electrostatic potential ϕ of the zonal flow and the ion temperature gradient (ITG) turbulence obtained by the GKV *simulation for inward-shifted (left) and standard (right) model configurations of the Large Helical Device (LHD). Normalization is chosen as $e\phi L_n/T_e\rho_i$.*

Spatio-temporal profiles of the zonal-flow potential averaged on the flux surface are plotted in Fig. 2, where the coherent radial structure of the flux-surface averaged potential, $\langle\phi\rangle$ is clearly found in the inward-shifted case shown in the left panel. The zonal-flow amplitude generated in the inward-shifted case is much higher than that of the standard configuration shown in the right panel. Fluctuating components of $\langle\phi\rangle$ in the radial-temporal space dominate in the standard case. The larger zonal-flow generation in the inward-shifted case agrees with results from the linear analysis of the zonal-flow response [7–9], which predicts a larger zonal-flow response to a given source in neoclassically optimized helical configurations. The peak value of the time-averaged zonal-flow potential $\langle\phi\rangle \approx 4.5T_e\rho_i/eL_n$ for the inward-shifted plasma is about six times larger than the largest amplitude of $\langle\phi\rangle \approx 0.74T_e\rho_i/eL_n$ for the standard case. The stationary zonal flow strongly excited in the inward shifted case regulate the ITG turbulence, and leads to ion heat transport reduction.

Time-history of the ion heat transport coefficient χ_i is plotted in Fig. 3. Although the linear ITG instability grows slightly faster and causes the higher peak value of χ_i for the inward-shifted configuration than for the standard case, the time-averaged value of $\chi_i \approx 1.27\rho_{ti}^2 v_{ti}/L_n$ in the saturated ITG turbulence ($t > 60L_n/v_{ti}$) for the former case is about 30% smaller than that of $\chi_i \approx 1.78\rho_{ti}^2 v_{ti}/L_n$ for the latter one. The evident transport reduction in the inward-shifted case is attributed to the enhanced zonal flows in the optimized helical configurations for decreasing neoclassical ripple transport, which provides a physical explanation to the confinement improvement found in the inward-shifted LHD plasma. Obvious stationary zonal-flow structures and turbulent-transport reduction shown in Figs. 1–3 for the inward-shifted case were not found in our previous simulations using simpler model configurations [13].

3. Effects of Equilibrium Radial Electric Fields on Zonal Flows

The gyrokinetic theory on zonal flows in helical systems suggest further enhancement of

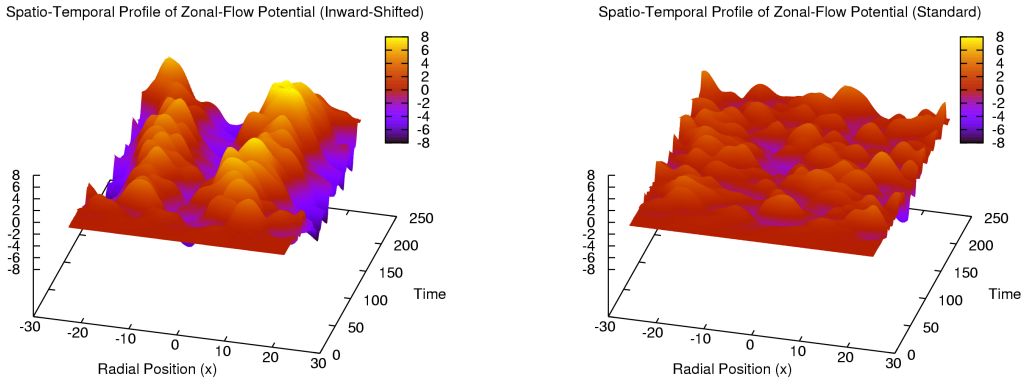

FIG. 2: Spatio-temporal profile of the zonal-flow potential in the ion-temperature-gradient turbulence for the inward-shifted (left) and the standard (right) LHD configurations.

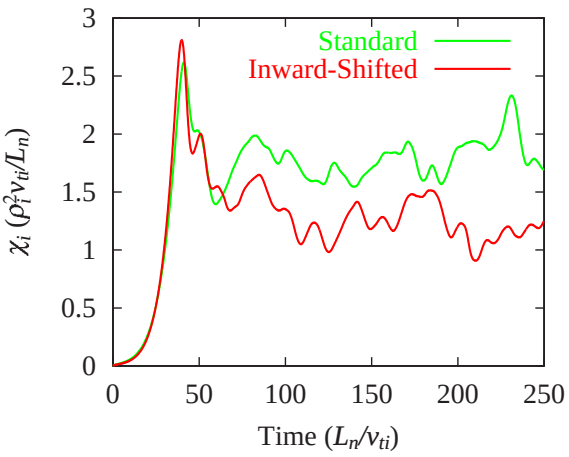

FIG. 3: Time-history of the ion heat conductivity χ_i for the inward-shifted (red) and the standard (green) LHD configurations.

zonal flows and resultant transport reduction, when the equilibrium radial electric field produces the poloidal $\boldsymbol{E} \times \boldsymbol{B}$ rotation of helical-ripple-trapped particles with reduced radial displacements [19, 20]. We have theoretically and numerically investigated the zonal-flow response in case with the radial electric field. The GKV code is newly extended so as to include the poloidally rotating $\boldsymbol{E} \times \boldsymbol{B}$ drift particles. In this section, enhancement of the zonal-flow response by the equilibrium radial electric field is confirmed by means of the new GKV simulations.

3.1. Theoretical Analysis

So far, we have neglected the equilibrium radial electric field (E_{r0}) which can be spontaneously generated in helical systems due to the ambipolar neoclassical particle transport. Further enhancement of zonal flows and resultant transport reduction are theoretically expected [20] when E_{r0} causes poloidal $\boldsymbol{E} \times \boldsymbol{B}$ rotation of helically-trapped particles with reduced radial displacements [19].

In this section, we assume E_{r0} to be uniform. In this case, regarding the ITG modes, E_{r0} just

gives the Doppler shift of the real frequency. Also, it has no contribution to zonal flows if the equilibrium is symmetric with respect to the field-line label α. When one considers the explicit α-dependence of the equilibrium field, however, the perturbed gyrocenter distribution function δf depend on α through the magnetic drift term even if the zonal-flow potential is independent of α. In helical systems, therefore, the $\boldsymbol{E}\times\boldsymbol{B}$ drift term associated with E_{r0} should generally be kept in the gyrokinetic equation in order to investigate the zonal-flow response in the case with the equilibrium radial electric field.

For the helical configuration with the single-helicity component, we have derived the response kernel of zonal flows in the long time limit [20],

$$\mathscr{K}_{Er} = \left[1+G+\frac{15}{8\pi}(2\varepsilon_h)^{1/2}\left(\frac{\varepsilon_t v_{ti}}{r\omega_\theta}\right)^2\left(1+\frac{T_e}{T_i}\right)\right]^{-1} \tag{2}$$

where the shielding term due to radial drift motions of the helical-ripple-trapped particles is inversely proportional to the square of E_{r0} with $\omega_\theta \equiv -cE_{r0}/rB_0$. We see that, as E_{r0} increases, the response kernel $\mathscr{K}_{Er}$ increases and approaches $1/(1+G)$ where G represents the ratio of the neoclassical polarization due to toroidally trapped ions to the classical polarization.

In helical configurations optimized for reduction of the neoclassical transport, such as the inward-shifted plasma in LHD, the enhancement of zonal-flow response due to E_{r0} is expected to work more effectively than in others because the neoclassical optimization reduces radial displacements of helically-trapped particles during their poloidal $\boldsymbol{E}\times\boldsymbol{B}$ rotation.

3.2. Simulation Model

The theoretical prediction about the effects of the equilibrium radial electric field on the zonal-flow response is examined by the newly-extended GKV simulation. In the present study, we solve the gyrokinetic equation modified for describing the collisionless damping of zonal flows with the equilibrium E_{r0} in the helical configuration with α-dependence,

$$\frac{\partial \delta f}{\partial t} + v_\parallel \boldsymbol{b}\cdot\nabla\delta f + \boldsymbol{v}_d\cdot\nabla\delta f - \mu\,(\boldsymbol{b}\cdot\nabla\Omega_i)\frac{\partial \delta f}{\partial v_\parallel} + \omega_\theta\frac{\partial \delta f}{\partial \alpha} = -\boldsymbol{v}_d\cdot\frac{e\nabla\langle\Phi\rangle}{T_i}F_M \tag{3}$$

where the field-aligned coordinates of $x = r - r_0$, $y = r_0[\theta - \zeta/q]$, and $z = \zeta$, are used with the field-line label $\alpha = \theta - \zeta/q$. We choose α so that $\boldsymbol{B} = \nabla\Psi_t\times\nabla\alpha$. In our previous simulations, we have employed the ballooning representation and the local flux-tube model around a single field line. On the other hand, the new simulation model including the poloidal $\boldsymbol{E}\times\boldsymbol{B}$ rotation of helically trapped particles is poloidally global. The equilibrium electric field is introduced as the fifth term on the left-hand-side of Eq.(3). We define the zonal-flow component of the electrostatic potential by $\langle\Phi\rangle$, so as to decouple components of unstable ITG modes that enter through the α-dependence, where the flux surface average is given by

$$\langle A\rangle = \int_{-N_\zeta\pi}^{+N_\zeta\pi} d\zeta \int_0^{2\pi} d\alpha \frac{A(\alpha,\zeta)}{B(\alpha,\zeta)} \Bigg/ \int_{-N_\zeta\pi}^{+N_\zeta\pi} d\zeta \int_0^{2\pi} d\alpha \frac{1}{B(\alpha,\zeta)}\,. \tag{4}$$

The toroidal extent of the simulation domain is denoted by $\pm N_\zeta\pi$ so that N_ζ/q is an integer. No magnetic shear of the confinement field is assumed ($\hat{s}=0$), since we still consider a radially-local region around $r = r_0$ where the magnetic shear on the zonal flow potential is expected to be small.

The electrostatic potential is given by the quasi-neutrality condition. For simplicity, we assume the hot electron limit of $T_i/T_e = 0$, and hence, the density perturbation vanishes in the quasi-neutrality condition. Thus, the electrostatic potential is simply given by

$$n_0(1-\Gamma_0)\frac{e\phi_{k_x,k_y}}{T_i} = \int J_0 f_{k_x,k_y} d^3v \tag{5}$$

where the Fourier component of δf and ϕ are represented by f_{k_x,k_y} and ϕ_{k_x,k_y}, respectively. Also, $\Gamma_0 = e^{-b}I_0(b)$ with $b = (k_\perp v_{ti}/\Omega_{i0})^2$ and $J_0 = J_0(k_\perp v_\perp/\Omega_{i0})$. The zeroth-order Bessel and modified Bessel functions are denoted by J_0 and I_0, respectively. The weak dependence on α and ζ of the arguments for J_0 and Γ_0 is neglected by using $\Omega_{i0} = eB_0/m_i c$. We also define $\Phi_{k_x,k_y} = J_0\phi_{k_x,k_y}$.

3.3. Simulation Results

The new GKV simulations of the collisionless damping of zonal flows are carried out for a model configuration with a single-helicity component of $L = l = 2$ and $M = 10$ with $\varepsilon_l = \varepsilon_t = 0.1$ and $(r_0/\varepsilon_t)(d\varepsilon_{l=2}/dr) = 2$. The following parameters are employed in numerical simulations: the minor radius $r_0 = 120\rho_i$, $k_x\rho_i = 0.131$, $q_0 = 1.5$, and $N_\zeta = 3$. The y and z coordinates of $-r_0\pi \le y < +r_0\pi$ and $-N_\zeta\pi \le z < +N_\zeta\pi$ are discretized by 128×1536 grid points, respectively. The velocity-space of $(v_\parallel, \mu)$ is represented by 256×48 mesh points. The y-derivative is calculated in the Fourier space of k_y. Here, as one of the normalization units, we employ the major radius R_0 instead of L_n.

Numerical simulations are carried out for $\omega_\theta/(v_{ti}/R_0) = 0$, $5/12$, $5/6$, and $5/4$, respectively. Time-history of the zonal-flow potential $\langle\phi_{k_x}(t)\rangle$ is plotted in Fig .4 for different ω_θ. For larger ω_θ, the first minimum value of $\langle\phi_{k_x}(t)\rangle$ before $t = 2R_0/v_{ti}$ increases. After the initial GAM damping ($t > 6R_0/v_{ti}$), the zonal-flow potential starts to oscillate. The oscillation period becomes shorter for larger ω_θ, and is about $4.2R_0/v_{ti}$ for $\omega_\theta/(v_{ti}/R_0) = 5/4$ which is a bit shorter than the poloidal rotation period $2\pi/\omega_\theta = 5.0R_0/v_{ti}$. More importantly, the time-averaged potential after the initial GAM damping is remarkably enhanced by introduction of the equilibrium radial electric field, which is consistent to the theoretical prediction. The time-averaged residual zonal-flow level for $\omega_\theta/(v_{ti}/R_0) = 5/4$ is about 2.5 times higher than that for $\omega_\theta/(v_{ti}/R_0) = 0$. The present GKV simulation results confirm the zonal-flow enhancement due to the equilibrium radial electric field. More detailed analysis of the residual level and the oscillation frequency found after the GAM damping is currently in progress and will be reported elsewhere.

4. Summary

In order to investigate effects of helical magnetic configurations and equilibrium radial electric fields on the ion temperature gradient (ITG) turbulence and zonal flows, we have performed gyrokinetic Vlasov simulations with the GKV code on the Earth Simulator. The simulation result obtained for the inward-shifted configuration of the Large Helical Device (LHD) manifests generation of large-amplitude stationary zonal-flow structures leading to significant turbulent-transport reduction [14], which was not so obviously shown in our previous simulations using simpler model configurations [13]. The present result confirms the theoretical prediction [7, 8] that helical configurations optimized for reducing neoclassical ripple transport can simultaneously improve the turbulent transport with enhancing zonal-flow generation, and also provides a possible explanation to the confinement improvement observed in the LHD experiments of inward plasma shift [12].

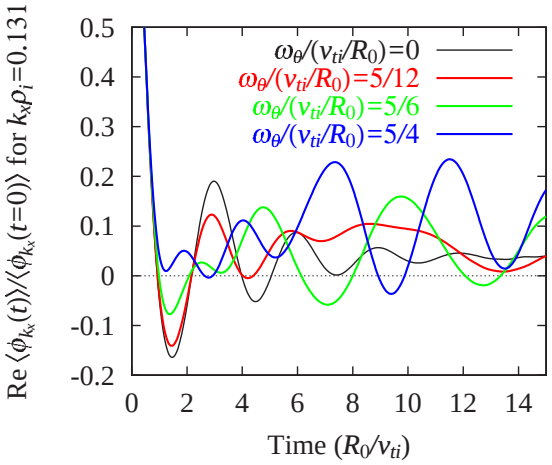

FIG. 4: Time-history of the zonal-flow potentials, $\langle\phi_{k_x}(t)\rangle$ obtained by the newly extended GKV *code for cases with equilibrium radial electric field. The poloidal rotation frequency of helical-trapped particles are changed as $\omega_\theta/(v_{ti}/R_0) = 0$, $5/12$, $5/6$, and $5/4$, respectively.*

Recent theoretical analysis [20] predicts further enhancement of zonal flows in the presence of equilibrium radial electric fields which produce poloidal $\boldsymbol{E}\times\boldsymbol{B}$ rotation of helical-ripple-trapped particles with decreased radial displacements. Thus, the anomalous transport is expected to be more effectively reduced by the equilibrium electric fields in neoclassically optimized helical configurations such as the inward-shifted LHD case. Enhancement of the zonal-flow response in case with the radial electric fields are also confirmed by means of the newly-extended GKV simulation code which introduces the poloidal rotation of $\boldsymbol{E}\times\boldsymbol{B}$ drift particles.

The present study demonstrates that a coupling of the neoclassical and turbulent transport mechanisms through zonal flows exists in helical systems, and that it is an important property of helical plasmas for investigating the confinement improvement.

Acknowledgments

The authors thank Dr. M. Yokoyama, Dr. S. Satake and Dr. H. Yamada for useful discussions on equilibria, stability, GAM oscillations, and transport properties of helical plasmas. This work is supported in part by grants-in-aid of the Ministry of Education, Culture, Sports, Science and Technology (No. 16560727, 17360445, and 17·05373), and in part by the National Institute for Fusion Science (NIFS) Collaborative Research Program (NIFS05KKMT001, NIFS06KTAT038, NIFS06KDAD006, NIFS06KNXN060, NIFS08KTAL06, NIFS08KNXN145, and NIFS08KDAD008). Numerical simulations are carried out by use of the Earth Simulator under the support by Japan Agency for Marine-Earth Science and Technology, and by use of the Plasma Simulator and the LHD numerical analysis system at National Institute for Fusion Science.

Reference

[1] HORTON, W., Rev. Mod. Phys. **71**, 735 (1999).
[2] DIAMOND, P.H., ITOH, S.-I., ITOH, K., HAHM, T.S., Plasma Phys. Control. Fusion **47**, R35 (2005).
[3] BRIZARD, A.J., HAHM, T.S., Rev. Mod. Phys. **79**, 421 (2007).

[4] ROSENBLUTH, R.M., HINTON, F.L., Phys. Rev. Lett. **80**, 724 (1998).
[5] WATANABE, T.-H., SUGAMA, H., Nucl. Fusion **46**, 24 (2006).
[6] WINSOR, N., JOHNSON, J.L., DAWSON, J.J., Phys. Plasmas **11**, 2448 (1968).
[7] SUGAMA, H, Watanabe, T.-H., Phys. Rev. Lett. **94**,115001 (2005).
[8] SUGAMA, H, Watanabe, T.-H., Phys. Plasmas **13**, 012501 (2006).
[9] FERRANDO-MARGALET, S., SUGAMA, H., WATANABE, T.-H., Phys. Plasmas **14**, 122505 (2007).
[10] MYNICK, H.E., Phys. Plasmas **13**, 058102 (2006).
[11] MOTOJIMA, O., et al., Nucl. Fusion **43**, 1674 (2003).
[12] YAMADA, H., et al., Plasma Phys. Control. Fusion **43**, A55 (2001).
[13] WATANABE, T.-H., SUGAMA, H., FERRANDO-MARGALET, S., Nucl. Fusion **47**, 1388 (2007).
[14] WATANABE, T.-H., SUGAMA, H., FERRANDO-MARGALET, S., Phys. Rev. Lett. **100**, 195002 (2008).
[15] FRIEMAN, E.A, CHEN, L., Phys. Fluids **25**, 502 (1982).
[16] BEER, M.A., COWLEY, S.C., HAMMETT, G.W., Phys. Plasmas **2**, 2687 (1995)
[17] SUGAMA, H., WATANABE, T.-H., Phys. Plasmas **11**, 3068 (2004).
[18] KURODA, T. et al., J. Phys. Soc. Jpn. **69**, 2485 (2000).
[19] MYNICK, H.E., BOOZER, A.H., Phys. Plasmas **14**, 072507 (2007).
[20] SUGAMA, H., WATANABE, T.-H., FERRANDO-MARGALET, S., Plasma Fus. Res. **3**, 041 (2008).